

## Figure Caption

Fig. 1.1 Wollaston Prism .....	2
Fig. 1.2 MacNeille polarizing beam splitter cube .....	3
Fig. 1.3 Polarized light separation of a sub-wavelength grating .....	4
Fig. 2.1 A general dielectric grating .....	8
Fig. 2.2 Schematic of a zero-order grating ( $p \ll \lambda$ ) with the polarized orientations of the incident electric field and definitions of rectangular grating parameters .....	9
Fig. 2.3 Effective refractive indices, $n_{TE}$ and $n_{TM}$ , versus fill factor $f$ .....	12
Fig. 3.1 (a) Schematics, and (b) photograph of an electron beam writer .....	20
Fig. 3.2 Schematic diagram of interferometric lithography .....	22
Fig. 3.3 Schematic diagram of UV-nanoimprint lithography .....	23
Fig. 3.4 Flowchart of fabricating sub-wavelength grating on quartz .....	26
Fig. 3.5 Interferometric lithography exposure setup .....	27
Fig. 3.6 Processing flow chart of master mold fabrication .....	28
Fig. 3.7 Flow chart of the PDMS mold fabrication .....	29
Fig. 3.8 Flow chart of sub-wavelength grating fabrication with UV-nanoimprint lithography .....	30
Fig. 3.9 Process setup and results of standard evaporation .....	33
Fig. 3.10 Process setup and results of oblique evaporation .....	33
Fig. 3.11 Schematic diagram of scanning electron microscope .....	34
Fig. 3.12 Concept of AFM and the optical lever .....	35
Fig. 3.13 Schematic diagram of the efficiency measurement setup .....	36

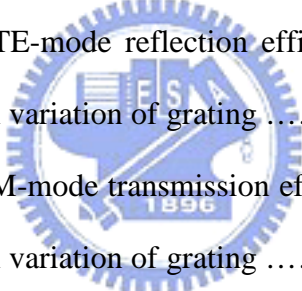
Fig. 4.1 Structure of the proposed sub-wavelength grating .....	39
Fig. 4.2 Simulated results of the proposed sub-wavelength grating .....	40
Fig. 4.3 Simulated results of TE-mode reflection efficiency versus wavelength of incident light with various periods of the sub-wavelength grating .....	42
Fig. 4.4 Simulated results of TM-mode transmission efficiency versus wavelength of incident light with various periods of the sub-wavelength grating .....	42
Fig. 4.5 Structure of the sub-wavelength grating with triangular profile .....	44
Fig. 4.6 Simulated results of TE-mode reflection efficiency versus wavelength of incident light with various structures of the sub-wavelength grating .....	44
Fig. 4.7 Simulated results of TM-mode transmission efficiency versus wavelength of incident light with various structures of the sub-wavelength grating .....	45
Fig. 4.8 Simulated results of TE-mode reflection efficiency versus wavelength of incident light with the line-width variation of grating .....	47
Fig. 4.9 Simulated results of TM-mode transmission efficiency versus wavelength of incident light with the line-width variation of grating .....	47
	
Fig. 5.1 AFM images of the photoresist grating with 200 nm period .....	50
Fig. 5.2 AFM images of the photoresist grating with 600 nm period .....	51
Fig. 5.3 SEM image of the top view of the photoresist grating with 600 nm period .....	51
Fig. 5.4 AFM images of the PDMS mold with 200 nm period .....	53
Fig. 5.5 AFM images of the PDMS mold with 600 nm period .....	54
Fig. 5.6 SEM results of the photoresist grating after the UV-nanoimprint (a) Sample I (b) Sample II .....	55
Fig. 5.7 Operation of imprint process .....	55
Fig. 5.8 Imprint result .....	56
Fig. 5.9 Imprint process using the proposed holder .....	56

Fig. 5.10 Uniformity of imprint by using a holder .....	57
Fig. 5.11 Uniformity of imprint improved by controlling the PDMS's thickness and the pressurized process .....	58
Fig. 5.12 Parameters of angled evaporation .....	59
Fig. 5.13 The proposed evaporated result .....	59
Fig. 5.14 The oblique evaporation result of sample I .....	61
Fig. 5.15 The oblique evaporation result of sample II .....	61
Fig. 5.16 Comparison of measured and calculated results of reflection efficiency versus wavelength of incident light .....	62
Fig. 5.17 Comparison of measured and calculated results of transmission efficiency versus wavelength of incident light .....	62
Fig. 6.1 Interferometric lithography with new incident angle $\theta$ .....	66
Fig. 6.2 The step and repeat method .....	67

